Journal of Structural Geology 131 (2020) 103939

Contents lists available at ScienceDirect

Journal of Structural Geology

journal homepage: http://www.elsevier.com/locate/jsg

Structural anisotropy: Using image analysis to quantify block-in-matrix fabrics

Alexander P. Clarke [a,*], Paola Vannucchi [a,b]

[a] Royal Holloway, University of London, Egham, TW20 0EX, UK
[b] Università di Firenze, Via la Pira, 4, 50121, Firenze, Italy

ARTICLE INFO

Keywords:
Anisotropy
Block-in-matrix
Mélange
Image analysis

ABSTRACT

Block-in-matrix rock assemblages — such as mélanges — are structurally complex units whose fabric is primarily defined, not by planar or linear features as most rock units are, but by the orientation and aspect ratio of irregularly shaped blocks. Despite this, previous attempts to quantitatively characterize mélange fabrics have predominantly focused on measuring the foliation using traditional techniques. Here we introduce a method of characterizing block-in-matrix fabrics using image analysis of field photos to discern the aspect ratios and orientations of blocks and define the *structural anisotropy* of the rock unit. We also include the software to calculate structural anisotropy and the trend of the fabric from image analysis data.

1. Introduction

Block-in-matrix rock assemblages (Raymond, 1984) — otherwise known as Bimrocks within the engineering geology field (Medley, 1994a) and including mélanges, olistostromes and large fault zones — are highly structurally complex units containing internal heterogeneities that make traditional structural geology techniques difficult to apply. Block-in-matrix fabrics are defined by the shape, orientation, size, size distribution, and proportion of their constituent blocks. Although these characteristics are the fundamental parameters of block-in-matrix rock units and their thorough description has been advocated by several workers (Wakabayashi, 2008; Medley and Zekkos, 2011; Grigull et al. 2012; Vannucchi et al. 2016), in practice they are rarely described systematically outside of the field of engineering geology (e.g. Lindquist, 1994). Most structural analysis of mélanges has focused chiefly on the orientation of the foliation (e.g. Kano et al. 1991; Singleton and Cloos, 2013; Fuentes et al. 2016). Foliation within these rock units is often controlled by the local stress field around relatively large blocks and does not accurately represent the regional stresses (e.g. Eden and Andrews, 1990; Shervais et al. 2011). Foliation may also be absent in many olistostromes or be difficult to discern in mélanges with a chaotic fabric (Clarke et al. 2018). Where foliation is present, it may be the result of a regional overprint and not the process that produced the rock unit or its block geometries, especially in the case of olistostromes which have been later deformed. As such, an alternative means of characterizing a block-in-matrix fabric and discerning its trend is required. Block shape, orientation, and proportion of mélanges has been examined to varying extents in the field of engineering geology where these factors influence the strength and stability of the rock mass and therefore the viability of engineering projects in areas where the bedrock has a block-in-matrix structure (e.g. Lindquist and Goodman, 1994; Riedmüller et al. 2001; Medley, 2002, 2004; Button et al. 2004; Kim et al. 2004; Sönmez et al. 2004; Roadifer et al. 2009). This paper introduces a method of using image analysis to quantitatively describe the shape and orientation of blocks in a block-in-matrix fabric to define the *structural anisotropy* of the rock mass. This approach is intended to be equally applicable to structural geologists and engineering geologists working on block-in-matrix rock units.

We have developed a methodology to quantitatively analyze the shape and orientation of blocks using image analysis to characterize mélange fabrics (Fig. 1). This methodology uses image analysis of field photos to assess the aggregated aspect ratios and orientations of a representative number of blocks to determine the generalized structural anisotropy of the fabric. In this context, structural anisotropy (SA) is defined as the difference between the proportions and the aspect ratios of blocks oriented parallel to and perpendicular to the orientation of the fabric. As an image analysis method, this technique measures structural anisotropy in two dimensions in the plane of the input photograph. This method is superior to separately describing the average or range of aspect ratios and their general trend because it allows recognition of

* Corresponding author.
E-mail address: alexander.clarke.2014@live.rhul.ac.uk (A.P. Clarke).

https://doi.org/10.1016/j.jsg.2019.103939
Received 12 March 2019; Received in revised form 8 November 2019; Accepted 25 November 2019
Available online 30 November 2019

systematic changes of aspect ratio with orientation as well as a quantification of the degree of alignment of the blocks.

While structural anisotropy of rocks has been explored, often in the form of shape-preferred orientation (SPO) analysis (e.g. Launeau and Robin, 1996; Herwegh and Handy, 1998; Cladouhos, 1999; Louis et al. 2005; Fuentes et al. 2016), it has typically focused solely on the number of fragments at a given orientation and has therefore under-emphasized the importance of different aspect ratios to the definition of structural anisotropy. Even more sophisticated approaches such as Launeau and Robin (1996, 2005) which count the number of intercepts between block shapes and a superimposed grid as the grid is rotated do not directly or intuitively represent aspect ratio, as is illustrated in Fig. 2II. This form of analysis has also rarely been used to characterize block-in-matrix rock units. Structural anisotropy is also not typically invoked in the context of meso-scale (10^{-2} – 10^{2} m) rock bodies, even in block-in-matrix rock units where particles may range in size from 10s of centimeters to hundreds of meters. The method detailed here provides a novel graphical approach which intuitively shows the structural anisotropy of a rock unit defined by the combined shape and orientation of its included fragments and provides a means of deriving a single value for such an anisotropy. Our method differs from — and may, for the situations described in this paper, be superior to — traditional analysis of shape preferred orientation (SPO) as it considers the aspect ratios of the blocks as a fundamental component of structural anisotropy.

This paper details the methodology for determining structural anisotropy from field photos using image analysis, describes how interpretation of structural anisotropy can be applied to the study of block-in-matrix rock units and illustrates this with examples from three mélanges, and discusses the strengths and limitations of this technique. This technique was developed to facilitate study of the Osa Mélange (Clarke, 2018), which lacks a well-developed foliation and displays a wide variety of block aspect ratios. The reproducibility of this method is tested by its application to the Gwna Mélange in north Wales (data from Clarke [2014]) and the Shimanto Belt in Japan (data from Takesue and Suzuki (2016)). The Gwna Mélange was chosen due to its strongly developed block-in-matrix texture, the presence of a strong matrix foliation lacking in the Osa Mélange, and the diversity of block shapes and aspect ratios. The Shimanto Belt was chosen for the visual contrast between blocks and matrix and the high quality interpreted aerial imagery provided by Takesue and Suzuki (2016). This method is especially applicable to aerial surveys using drone-derived imagery and may allow for rapid structural characterization over a large area in previously inaccessible locations.

2. Methodology for determining structural anisotropy

Structural anisotropy can be calculated using image analysis of a suitable photograph (Fig. 1). The software and a step-by-step guide to calculating structural anisotropy and plotting structural anisotropy diagrams can be found in Appendix A.

Determination of structural anisotropy requires an input image — typically a photograph — upon which image analysis can be performed (Fig. 1). This image should clearly show the block-in-matrix texture and contain a sufficient number of blocks to show a representative range of aspect ratios and orientations; this number will depend on the variability of block parameters and must be a judgement of the practitioner, but will usually contain no less than two examples of any major block population and the number of examples of each block population must be approximately in proportion with their occurrence in the input photograph. In cases where block margins are covered with

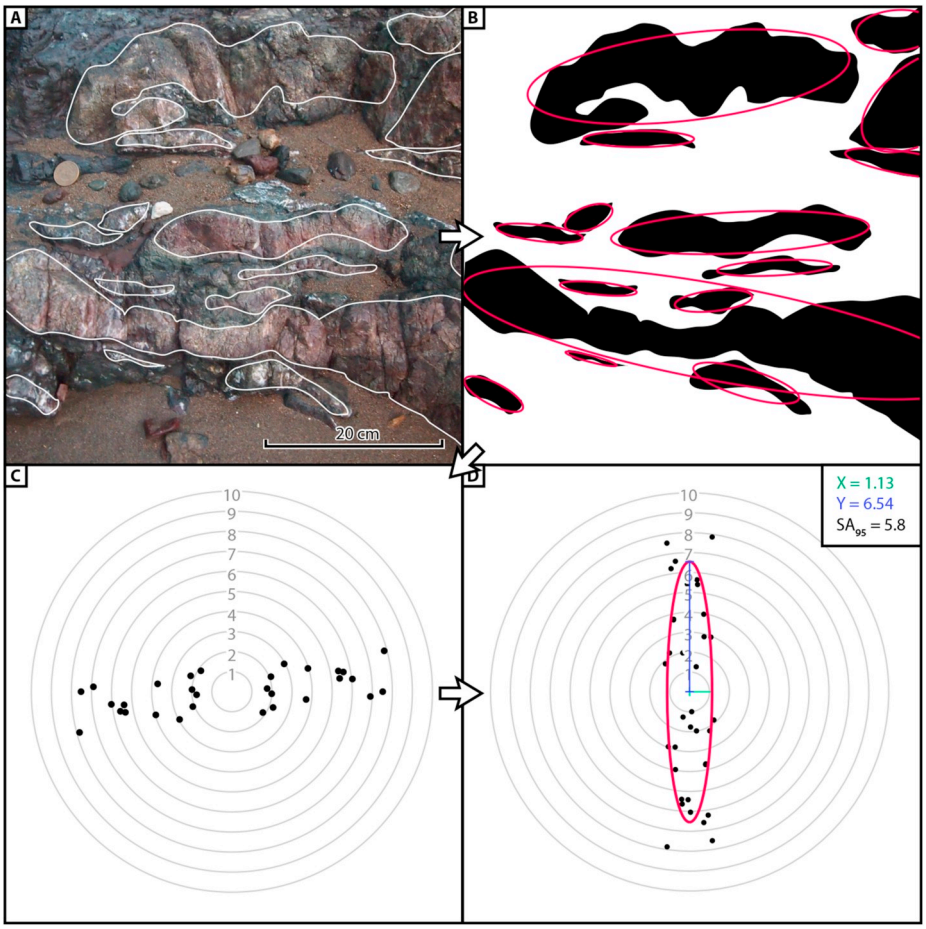

Fig. 1. Process of discerning structural anisotropy. **A:** First, block outlines are identified on a photograph. **B:** These outlines are analysed by image analysis software which fits ellipses to each block. **C:** Aspect ratio and orientation are plotted on a radar diagram to produce a cloud of data-point representing the general trend of the block-in-matrix fabric. **D:** Since no orientation marker is present in the photograph, the data cloud is detrended to remove the camera bias and an ellipse is plotted at the 95th percentile of the data cloud to produce the SA_{95} value (SA value calculated as SA = Y/X: X = 1.13, Y = 6.54, SA = 6.54/1.13 = 5.79).

loose debris, the user may have to erode the block contacts to ensure separation can be seen in the photograph. To avoid distortions, this photograph should ideally be taken orthogonal to the rock surface being shown and care should be taken to avoid optical distortions within the camera, such as barrel distortion. Images that may have been digitally distorted, such as georeferenced satellite imagery or panoramas constructed from multiple photographs, should be avoided. Ideally, all photos should be taken in the same orientation (e.g. camera oriented vertically above the outcrop) to enable accurate comparisons in the case when anisotropy varies in three dimensions. If this technique is being used to characterize the trend of the fabric — e.g. over a mapped area — a compass or other oriented object should be visible in the frame of the photo to allow correct orientation of the image. The precision and accuracy of this technique is limited by the quality of the input photograph and photographs showing a high degree of perspective may be unsuitable for this approach.

For the purposes of this method, blocks are defined as any contiguous object exhibiting a lithological or rheological contrast with its surrounding material and boundaries characterized by sharp, well-defined discontinuities. Typically, "blocks" will refer to fragments of one lithology included within a matrix of another lithology where a rheological contrast exists between the two components. However, "blocks" may also refer to lithologically distinct fragments without a notable rheological contrast between blocks and matrix — e.g. where lithication of the matrix concurrent with weakening of the block leads to a reduction of the rheological contrast — or lithologically homogenous rock units containing fragments more indurated than the matrix — e.g. where strain localization in an anastomosing fracture network leads to shear weakening around more obdurate phacoids. Note that blocks may be composed of more than one lithology, especially in cases where blocks are fault-bounded slices of a previously-intact stratigraphy. Following the Penrose definition of "mélange" (Silver and Beutner, 1980), this method can also be applied to "block-on-block" textures (Fig. 4a) and internally fragmented blocks (Fig. 4d). As demonstrated by Medley and Lindquist (1995), block-in-matrix textures are approximately fractal, meaning that the scale of observation determines which fragments are termed "blocks". As this method is scale-independent, "blocks" may refer to fragments of any scale which are clearly discernable in the input photograph.

The outline of these blocks must then be carefully traced using graphics software (e.g. Adobe Illustrator) — with care given to ensure blocks do not touch — to produce a two-tone image showing the shape of the blocks. It is not necessary to trace every block contained within the frame of the photograph providing a representative portion of the image — containing all major block populations in proportion to their occurrence in the photograph — is covered. Care must be taken to faithfully reproduce the geometries of the blocks and not favor blocks in certain orientations. Image analysis software (e.g. ImageJ) should then

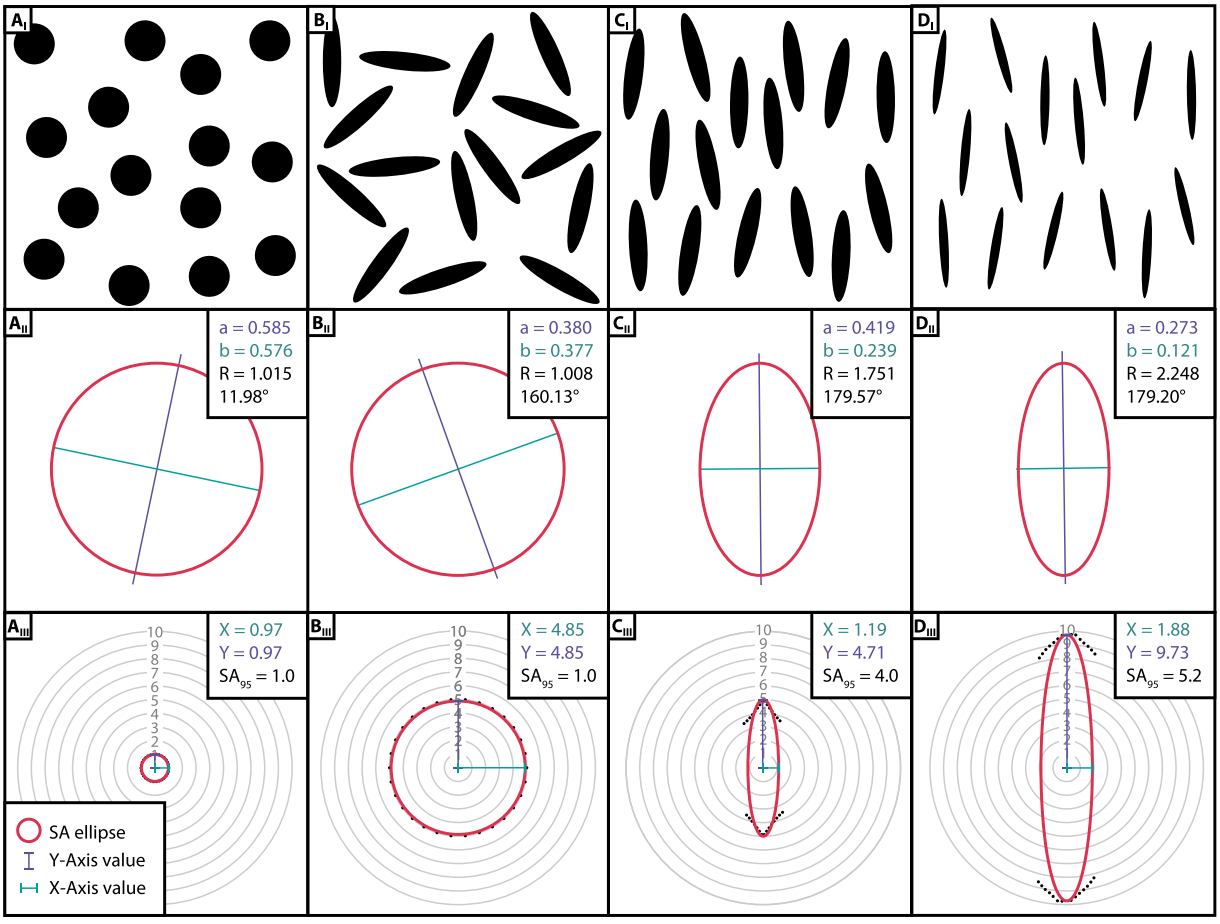

Fig. 2. Examples of structural anisotropy for synthetic data. Panels I show the synthetic input data, panels II show the shape-preferred orientation calculated using the software from Launeau and Robin (1996) for comparison to our structural anisotropy method (a = long axis, b = short axis, R = ratio between a and b; a and b values given in arbitrary units), and panels III show the structural anisotropy diagrams. SA value calculated as SA = Y/X. A: Circular blocks with an aspect ratio of 1:1 resulting in an SA_{95} value of 1.0 (X = 0.97, Y = 0.97, SA = 0.97/0.97 = 1.0). B: Elongate blocks with aspect ratios of 5:1 oriented so that no orientation is favoured, resulting in an SA_{95} value of 1.0 (X = 4.85, Y = 4.85, SA = 4.85/4.8 = 1.0). C: Elongate blocks with aspect ratios of up to 5:1 with a strong preferred orientation resulting in an SA_{95} value of 4.0 (X = 1.19, Y = 4.71, SA = 4.71/1.19 = 4.0). D: More elongate blocks with aspect ratios approaching 10:1 with a strong preferred orientation similar to C resulting in an SA_{95} value of 5.2 (X = 1.88, Y = 9.73, SA = 9.73/1.88 = 5.2).

be used to analyze the shape of these blocks. Blocks which are truncated by the frame of the photograph should be excluded from analysis.

The two parameters required to determine structural anisotropy are the aspect ratio and the orientation of the long axis of each of the blocks (Fig. 2). This should be plotted on a polar plot with orientation on the radial axis and aspect ratio on the circumferential axis. The data should be duplicated with 180° added to the orientation data to represent the bi-directionality of this data; the unidirectionality of some structural measurements does not contribute to structural anisotropy and is therefore ignored. The plotted data will produce an elliptical cloud of data points representing the generalized shape and orientation of the blocks (Fig. 2). If the photograph is geographically oriented (e.g. there is a compass or other oriented object within the frame of the photograph), this data cloud should be rotated to match this orientation.

If the image is not geographically oriented, this data cloud should be detrended (i.e. rotated so that the unknown trend is represented as if it were oriented N – S) to remove the artefact of the camera orientation relative to the rock fabric (Fig. 1c – d). Detrending is accomplished by rotating the orientation of the data until a minimum spread on the x-axis is reached. This is calculated as the difference between the sums of X-axis positions where X is negative and where X is positive, when only the pre-doubled data is considered. Detrending can be used to rotate the data cloud such that the maximum spread of data is in the plane of the Y-axis which can be used to aid comparison between differently oriented fabrics and it should always be used where the orientation of the fabric is unknown. It is also necessary for quantification of structural anisotropy.

To extract a single value for structural anisotropy from this cloud of data, an ellipse must be plotted which encloses the majority of the data cloud while excluding outliers (blocks with uncommon shapes and orientations which do not match the general trend). The semi-axes of this ellipse — referred to as the "structural anisotropy ellipse" — is defined by a percentile of the spread of data along the X and Y axes in a detrended diagram. The percentile chosen should reflect the number of data points and should be consistent between all images being compared; this percentile should be declared when reporting values from this technique, for example, if the 95th percentile is used, the value reported is the SA_{95} value, whereas if the 99th percentile is used, the value is the SA_{99} value. The 95th percentile is generally appropriate for images containing 10s of blocks, while the 99th percentile may be more appropriate where images contain 100s or 1000s of blocks. Greater numbers of blocks analysed reduces the uncertainty in this method and so the practitioner should aim to analyze the maximum number of blocks that is practical. The aspect ratio of the resultant ellipse is taken as the "structural anisotropy value". Where images are geographically oriented, the orientation of the long-axis of the structural anisotropy ellipse defines the trend of this fabric and should be reported alongside the structural anisotropy value.

3. The structural anisotropy ellipse

The structural anisotropy diagram (Fig. 2III) provides a highly visual means of representing block-in-matrix fabrics. Fig. 2 shows structural anisotropy in synthetic data to show how orientation and aspect ratio — two of the primary parameters in describing a block-in-matrix fabric — are presented in these diagrams. Fig. 2a shows circular blocks, i.e. without alignment, even though an orientation value is assigned to them by the image analysis software due to error inherent in representing a circular shape with square pixels. Since circles have an aspect ratio of 1:1, they plot at aspect ratio = 1 on the diagram, producing a structural anisotropy ellipse that is also circular, giving an SA_{95} value of 1. Fig. 2b shows elongate blocks (aspect ratio = 5:1) oriented such that no orientation is favoured. This produces a structural anisotropy diagram where all the blocks plot at aspect ratio = 5 and are evenly spaced around the diagram. Therefore, the structural anisotropy ellipse is once again circular, giving an SA_{95} value of 1. In both cases, the structural anisotropy value remains the same despite the differences in aspect ratios. This is because both cases lack a preferred orientation. The structural anisotropy value is therefore controlled not by the aspect ratios of the blocks directly, but the relationship between the aspect ratios of blocks in different orientations.

Fig. 2c shows elongate blocks (aspect ratio = 3.5:1–5:1) oriented with a moderate preferred orientation (N – S). In this case, the blocks plot around aspect ratio = 5 on the structural anisotropy diagram but are clustered towards the N and S of the diagram, therefore producing an elongated structural anisotropy ellipse and giving an SA_{95} value of 4.0. Fig. 2d shows similar elongate blocks with a higher aspect ratio (aspect ratio = 8.2–9.8) and a strong preferred alignment resulting in an SA_{95} value of 5.2.

The structural anisotropy ellipse is comparable to the ellipse of mechanical anisotropy (Buczek and Herakovich, 1985). The mechanical anisotropy ellipse represents the strength or seismic wave velocity at each orientation around the sample and is constructed by fitting an ellipse to this data. In contrast, the structural anisotropy ellipse encloses the cloud of data-points, exclusive of outliers. This is done to account for the significantly greater degree of scatter in the structural data.

The structural anisotropy ellipse is also similar in meaning to shape-preferred orientation ellipses such as those drawn by the software of Launeau and Robin (1996)(Fig. 2II). The trends of these ellipses in oriented diagrams are likely to be approximately parallel; however, as shape-preferred orientation does not consider aspect ratio as a fundamental component, the shapes and sizes of these ellipses may differ significantly. This can be seen in a comparison between the results of shape-preferred orientation (Fig. 2II) and structural anisotropy (Fig. 2III) where shape-preferred orientation shows the approximately circular ellipse for the randomly oriented synthetic data (Fig. 2a and b) and an elongated ellipse for the similarly oriented synthetic data (Fig. 2c and

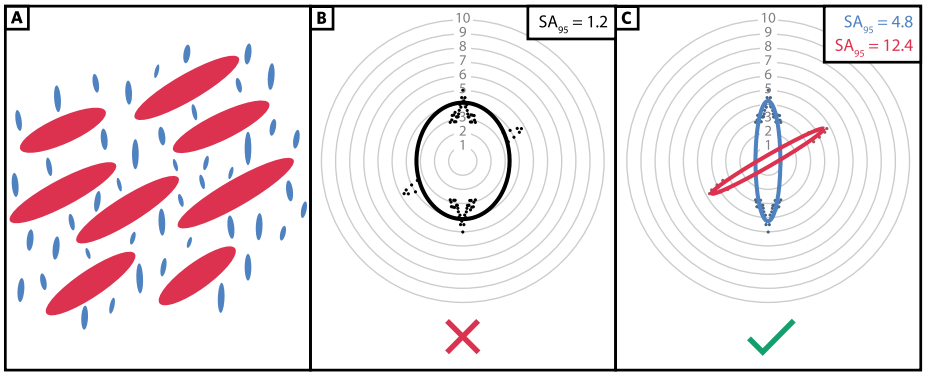

Fig. 3. Different domains within an image showing two distinct orientations and **A:** how not to characterize this using structural anisotropy (X = 3.23, Y = 4.03, SA = 4.03/3.23 = 1.2), and **B:** how to correctly characterize it (Blue: X = 0.84 Y = 4.05 SA = 4.05/0.84 = 4.8; Red: X = 0.36 Y = 4.52 SA = 4.52/0.36 = 12.4).

d) but does not distinguish between the different aspect ratios of the blocks.

This method of determining structural anisotropy is entirely independent of scale. In this case, "block" simply refers to any coherent clast with boundaries traceable at the scale of the input photograph and does not denote clasts of a certain size-range. This method also cannot distinguish between multiple domains with different orientations; therefore the practitioner must discriminate these zones and analyze each separately (Fig. 3).

It must be noted that — as with all image analysis of photographs — this method is inherently two-dimensional. As rock fabric is three-dimensional and the geometries of blocks in a mélange varies in three dimensions, the structural anisotropy ellipse produced by this method represents a cross-section through the structural anisotropy ellipsoid of the mélange fabric. The structural anisotropy ellipse and SA value therefore represent the structural anisotropy of the rock unit in the plane of observation. The semi-axes of the structural anisotropy ellipsoid can be approximated by producing structural anisotropy ellipses in three — ideally mutually perpendicular — orientations where one semi-axis is ideally parallel to the orientation of the fabric. Other techniques, such as that developed by Robin (2002), may be used to calculate the structural anisotropy ellipsoid from surfaces which are not mutually perpendicular. However, this three-dimensional analysis may not be practicable unless the practitioner artificially erodes three surfaces in compatible orientations or where coincidence has produced an outcrop with these correctly oriented surfaces. In this case, stereological techniques (e.g. Medley, 1994b) may be sufficient to estimate the three-dimensionality of the observed fabric. Despite the limitations inherent in two-dimensional analysis of a three-dimensional fabric, we believe that the two-dimensional analysis detailed in this approach provides valuable results for a broad range of applications.

4. Examples

4.1. Example 1: Osa Mélange, Costa Rica

The Osa Mélange, located in southwest Costa Rica, is an accreted unit of oceanic olistostromes, debris flows, and turbidites that has undergone intense deformation at a shallow depth within the Middle America Subduction Zone (Vannucchi et al. 2006; Buchs et al. 2009; Clarke et al. 2018). It consists of blocks of basalt, chert and carbonate within a volcanoclastic pelitic matrix and blocks generally range in size from 10^{-2} – 10^{2} m. This mélange contains packages exhibiting notable differences in average aspect ratio and preferred orientation, with some packages containing high aspect ratio (up to 11:1) blocks with a strong preferred orientation and visible folding, and other packages displaying low – moderate aspect ratio (generally up to 4:1 with outliers up to 8.5:1) blocks and very weak preferred orientation.

Much of the Osa Mélange lacks a defined foliation in either the matrix or the blocks and, where present, any foliation is weakly developed. The presence, orientation, and aspect ratio of the blocks are the overwhelmingly dominant feature in this mélange and, as such, traditional methods of characterizing the fabric of a rock unit — such as measurement of planar/linear structures using a compass-clinometer and representation of this data using a stereonet — are difficult to apply and are less appropriate to characterize the fabric. While these structures — where they are present — may still be used to identify the 3D orientation of planar features — especially foliation in the matrix — and to determine the deformation history (e.g. Vannucchi et al. 2006), they cannot be used to comprehensively characterize the block-in-matrix fabric. Aspect ratio and orientation of the blocks are more useful descriptors of the fabric than dip and strike of foliation. The structural anisotropy diagram therefore represents this mélange fabric more effectively and makes structural

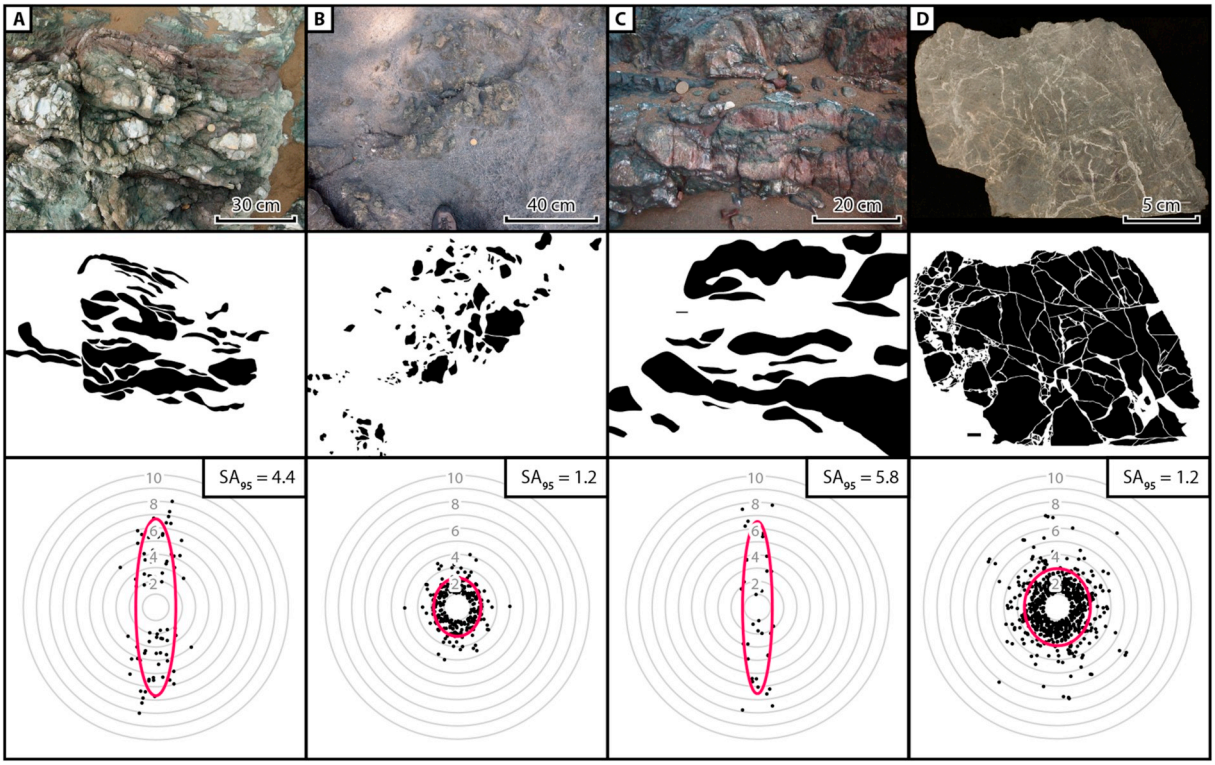

Fig. 4. Examples of structural anisotropy analysis performed on photos from the Osa Mélange (Clarke, 2018). The structural anisotropy diagrams are shown detrended as no orientation data is available for these photographs. **A:** The process is applied to a challenging outcrop photo where care is taken to avoid exaggerating block shape due to perspective (X = 1.51, Y = 6.67, SA = 6.67/1.51 = 4.42). **B:** Complex block-in-matrix structure represented using this method (X = 1.79, Y = 2.21, SA = 2.21/1.79 = 1.23). **C:** High aspect ratio aligned blocks represented using this method (X = 1.13, Y = 6.54, SA = 6.54/1.13 = 5.79). **D:** This process is applied to a cut surface of a single internally brecciated block, allowing for 100% coverage of the image and producing high quality data (X = 2.47, Y = 2.92, SA = 2.92/2.47 = 1.18).

characterization possible in areas where no planar structures exist. Using structural anisotropy, the weak preferred alignment of Fig. 4b and Fig. 4d can be detected. Identification and quantification of weak fabrics in block-in-matrix textures is a key strength of this methodology. This method can also quantify the in-plane preferred orientation in rock units with moderate – strong preferred orientation (e.g. Fig. 4a and Fig. 4c) at a higher precision than measuring block margins or estimating block axes in the field can accomplish. In addition to outcrop photographs, this method may be applied to internal fragments or included blocks within an ex-situ hand specimen; Fig. 4d therefore shows an example of structural anisotropy analysis performed on a cut surface of a single brecciated block.

4.2. Example 2: Gwna Mélange, Wales

The Gwna Mélange — located on Anglesey and the Llŷn Peninsula in north Wales, UK — is a late Neoproterozoic – early Cambrian accreted package consisting of tectonically dismembered sections of oceanic crust (Kawai et al. 2008) and olistostromes (Wood, 2012). The area of Llanbadrig, on the northern coast of Anglesey, contains a deformed olistostrome displaying remarkable block-in-matrix texture and consisting of blocks of variably sideritised limestone, red chert, and quartzite in a pelitic matrix (Wood, 2012). The region displays a strong NW – SE structural trend consistent with the closure of the Iapetus Ocean (Gibbons and McCarroll, 1993). The strong foliation which cuts the matrix here tortuously deflects around blocks, sometimes rotating as much as 90° in the space of a meter.

Despite the matrix of the Gwna Mélange possessing a strong pervasive planar foliation, the greatest variation in the fabric of the matrix — varying on the scale of ~10 m — is block aspect ratio and the degree of preferred alignment. The Gwna Mélange therefore provides an ideal test of the broader applicability of the structural anisotropy method beyond the Osa Mélange. Structural anisotropy effectively represents this variation in block shape and orientation (Fig. 5) and, when the structural anisotropy diagrams are oriented to reflect the compass orientations of the blocks, provides an intuitive visualization of

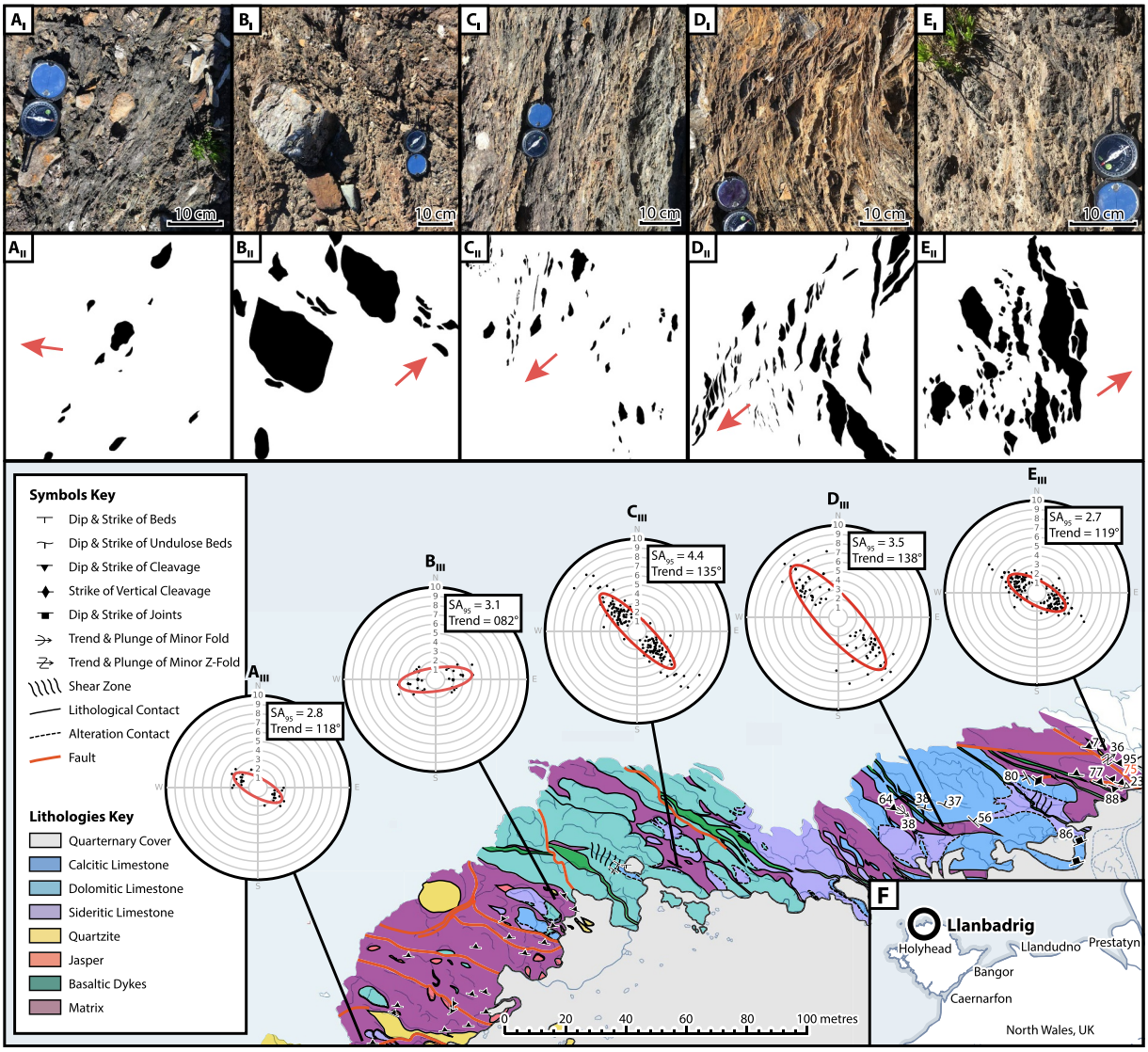

Fig. 5. Detailed geological map of the Gwna Mélange at Llanbadrig, northern Anglesey (Clarke, 2014) with structural anisotropy diagrams showing the variation in the block-in- matrix texture within this small area. A: Low – moderate block aspect ratios and low block proportions (X = 1.04, Y = 2.91, SA = 2.91/1.04 = 2.80). B: Low – moderate block aspect ratios where blocks are partially obscured by loose rocks (X = 1.27, Y = 3.99, SA = 3.99/1.27 = 3.14). C: Low – moderate block aspect ratios where high aspect ratio blocks show high degree of alignment (X = 1.27, Y = 5.62, SA = 5.62/1.27 = 4.43). D: Moderate – high aspect ratio blocks with high block proportions in mélange cut by shear zone (X = 2.09, Y = 7.40, SA = 7.40/2.09 = 3.54). E: Low – high block aspect ratios with moderate alignment (X = 1.31, Y = 3.50, SA = 3.50/1.31 = 2.67).

the fabric. Fig. 5a and 5b represent areas with low block proportions and where blocks exhibit low – moderate aspect ratios; however, the alignment of these blocks remains strong. Fig. 5c represents an area between several mega-blocks (>100 m in length) where the matrix features highly elongate blocks showing strong alignment. Fig. 5d and 5e shows high proportions of blocks with high aspect ratios and moderate – strong alignment.

4.3. Example 3: Shimanto Belt, Japan

The Shimanto Belt is a Cretaceous – early Cenozoic accretionary complex exposed along the south-western margin of the Japanese islands of Shikoku and Kyushu. This belt is predominantly composed of flysch but also contains several mélange zones which predominantly contain blocks of metabasalt and sandstone within an argillaceous matrix (Suzuki and Hada, 1979; Raimbourg et al. 2017). In the Shiofuki-iwa area studied by (Takesue and Suzuki, 2016), the mélange consists of lens-shaped sandstone blocks exhibiting pinch-and-swell structures within a mudstone matrix. These blocks are interpreted to be the result of tectonic dismemberment at a shallow depth within the subduction zone prior to lithification (Takesue and Suzuki, 2016).

Takesue and Suzuki (2016) characterized a section of the Shimanto Belt mélange in the Shiofuki-iwa area and included high quality interpreted aerial photographs taken with the use of a drone. These aerial images are ideal for the application of the structural anisotropy technique. The sections of the Shimanto Belt photographed by Takesue and Suzuki (2016) all exhibit high aspect ratios and a moderate – strong preferred alignment. It also exhibits a strong S–C foliation to which the long-axes of the blocks are approximately aligned. Fig. 6 shows the interpreted drone photographs from Takesue and Suzuki (2016) and our structural anisotropy diagrams produced from them. In these images, structural anisotropy analysis reveals variation in the degree of alignment which is not obvious by visual assessment. Fig. 6a shows a moderate structural anisotropy despite high aspect ratios due to the

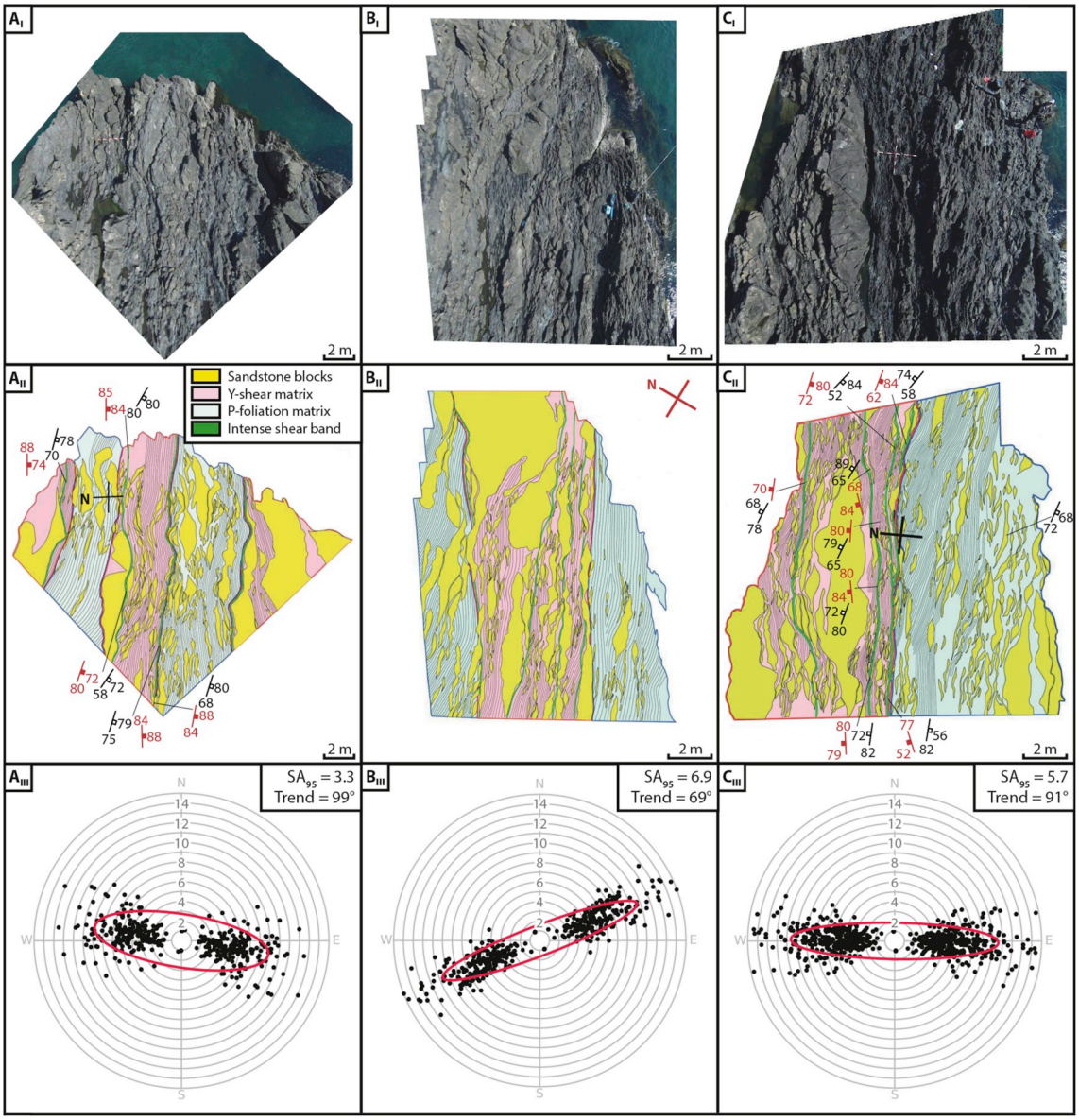

Fig. 6. Structural anisotropy analysis of interpreted drone-derived aerial imagery of the Shimanto Belt mélange from Takesue and Suzuki (2016). The reader is directed to Takesue and Suzuki (2016) for an explanation of their analysis. A: Despite high aspect ratios, the variability in block orientations produce a moderate value of structural anisotropy (X = 2.71, Y = 8.93, SA = 8.93/2.71 = 3.30). B: High aspect ratios and strong block alignment produce a high value of structural anisotropy (X = 1.54, Y = 10.66, SA = 10.66/1.54 = 6.92). Orientation (red cross) estimated from Takesue and Suzuki (2016) Fig. 4. C: High aspect ratios and strong block alignment produce a high value of structural anisotropy (X = 1.86, Y = 10.59, SA = 10.59/1.86 = 5.69).

variability in block orientations. In contrast, Fig. 6b and c shows higher structural anisotropy with similarly high aspect ratios due to stronger alignment of the blocks.

5. Relationship to mechanical anisotropy

The structure of a rock mass is a first-order control on its mechanical anisotropy (including strength and elastic anisotropies), as these structures control the location and orientation of flaws, concentrate stresses, and impede the propagation of seismic waves (Louis et al. 2005). Therefore, structural anisotropy — defined by the shape and orientation of the structures in the rock mass — is a key indicator of other forms of material anisotropy and has been shown to influence the deformation style within the rock mass (e.g. Butler et al. 2008). As the shape and orientation of these structures also define the fabric of the rock — with higher aspect ratio features generally aligning parallel to sub-parallel with the fabric — characterization of the rock's structure provides an approximation of the orientation and comparative magnitude of the rock's mechanical anisotropy.

Typically, mechanical anisotropy is directly measured in laboratory conditions by either destructive deformation experiments (Coli et al. 2008; Forbes Inskip et al. 2018) or by propagating acoustic waves through the material (e.g. Svitek et al. 2014). Both methods typically require samples <10s of centimeters in size. Alternatively, *in situ* measurements of elastic anisotropy may be conducted at a macro- and mega-scale from the travel time of seismic waves through the rock mass (Savage, 1999; Tepp et al., 2018). Structural anisotropy of field photos allows assessment of a rock's anisotropy at a meso-scale, which cannot be practically achieved using existing methods. Using structural anisotropy as a proxy for mechanical anisotropy, the difference in strength between different orientations of the mélange fabric can be estimated, even in cases where traditional methods of determining mechanical anisotropy cannot be used, for example, due to the scale of the blocks. This technique is complimented by analysis of the block proportions (e.g. Medley, 1994b; 1997; Haneberg, 2004) — which may also be accomplished by image analysis — which also contributes to the mechanical anisotropy of the rock mass.

6. Considerations and limitations

This methodology is limited to only two-dimensional sections of the rock mass, as true three-dimensional images cannot be obtained by photograph. This limitation is common to all image analysis of photographs, as well as to the sub-disciplines of microtectonics and remote-sensing. As such, the practitioner should be cognizant that this method measures structural anisotropy *in-plane* and does not necessarily represent the true semi-axes of the structural anisotropy ellipsoid of the rock's three-dimensional fabric. Despite this, two-dimensional fabric analysis is valuable to the study of fabric variations over a mapped area, as a proxy for the mechanical anisotropy in that plane, and as a simple method for rapidly characterizing the rock unit's fabric. Approximations of the three-dimensional fabric ellipsoid may be constructed from two-dimensional sections using the technique of Robin (2002).

The accuracy and precision of this method are strongly dependent on the interpretation of the practitioner, as the precise location of blocks and block boundaries may be difficult to determine due to weathering or visual similarities between the block and matrix lithologies. Therefore, care must be taken to fairly represent all block sizes, orientations and aspect ratios within the frame of the photograph.

This method does not consider the proportions of blocks and matrix, which — in addition to the shape and orientation of the blocks — also represent a key first-order control on material anisotropy. While image analysis has the capacity to quantify the area of the image covered by blocks and the area covered by matrix, this would require that all blocks within the frame of the photograph be traced; in most cases it is not practical to expect that all blocks will be recognized and traced with sufficient accuracy to allow this analysis. In many cases, there may be significantly more blocks than can practically be traced, and often regions of the photograph are obscured by foliage, loose stones, soil, or scale and orientation indicators.

This method is scale-independent and can therefore be applied to any rock unit or portion of a rock unit containing blocks. This method is therefore flexible enough to be applied to a wide range of block-in-matrix rock units and is suitable for analysis at a wide range of scales; it may similarly be used to compare the structural anisotropy of a single rock unit across scales. Unless comparison between scales is the objective of the study, care should be taken not compare structural anisotropy using photographs at different scales, i.e. results from a hand-specimen-sized cut block should not be compared with an outcrop photograph with a field-of-view of several meters or an aerial photograph with a field-of-view of tens of meters unless the difference in scale is explicitly stated.

Whilst a relationship exists between block preferred alignment and elongation and the amount of strain experienced by the rock unit, this relationship is not simple. Similar relationships exist between strain and shape-preferred orientation and have been discussed extensively (see Cladouhos, 1999). The orientation of the three-dimensional structural anisotropy ellipsoid may represent the orientation in which the rock unit underwent strain, however the magnitude of structural anisotropy does not necessarily represent the amount of strain experienced. The magnitude of structural anisotropy may underestimate the amount of strain if strain is localized in the matrix or overestimate the amount of strain if blocks are produced by boundinage and dismemberment of previously bedded rock units. As such, the structural anisotropy method should be used alongside existing techniques to discern the amount of strain. Similarly, structural anisotropy analysis does not replace standard visual assessment of an outcrop to identify other structural features including asymmetry of blocks.

Although structural anisotropy analysis represents the fabric of a block-in-matrix rock unit better than simple measurements of planar and linear surfaces with a compass-clinometer, it does not fully replace such traditional techniques as part of a holistic assessment of the rock unit. The structural anisotropy technique does not record the dip of the fabric which may be assessed by measurement of the foliation, and discordance between the strike of the foliation and the trend of the structural anisotropy may reveal a tectonic overprint or shear-zone kinematics (Herwegh and Handy, 1998).

7. Conclusions

The structural anisotropy technique allows quantification of block-in-matrix fabrics from field photos. The fabric of block-in-matrix rock units — such as mélanges and olistostromes — is often difficult to accurately characterize and measure due to the high degree of foliation deflection around blocks. Image analysis of these field photos can be used to determine the orientation and aspect ratios of each of the blocks, from which a structural anisotropy diagram can be constructed which visually represents the block-in-matrix nature of the mélange fabric. Blocks are essential to characterize the nature and structure of mélanges.

On the first order, the fabric of a mélange is described by the arrangement of its blocks — not by any planar or linear structures that may cut the mélange — therefore, the structural anisotropy diagram represents this fabric in a manner which is more appropriate and representative than stereonets of its foliation. Our structural anisotropy method differs from existing shape-preferred orientation methods as it considers block aspect ratio as a fundamental component, making it more representative of the shape of the block arrays and a more intuitive graphical depiction of the rock fabric.

In addition to visually representing the fabric of a block-in-matrix rock unit, structural anisotropy may also represent an effective proxy for material anisotropy as the structural components in the rock mass strongly influence the variations in mechanical properties. As such, the

orientation and relative magnitude of mechanical anisotropy can be estimated from the structural anisotropy. This technique may be used in scenarios where material anisotropy cannot be measured experimentally due to the scale of observation, logistical difficulties, or expense.

The dominant structural component in a mélange unit is its block arrays, and not planar or linear features as is typical of other rock units. In mélanges, planar and linear features are commonly observed to bend around blocks or be deflected by blocks, and so may be unreliable for analysis of the regional fabric. We therefore propose the adoption of the structural anisotropy technique to quantitatively characterize block-in-matrix fabrics. Use of this method could supplement traditional structural geology techniques such as measurement of foliations with a compass-clinometer or be used in situations where the traditional methods cannot be used.

Declaration of competing interest

The authors declare that they have no known competing financial interests or personal relationships that could have appeared to influence the work reported in this paper.

Acknowledgements

We thank Norito Takesue and Shigeyuki Suzuki for permission to reproduce their interpreted aerial images and for providing their original photographs. We also thank two anonymous reviewers for their valuable suggestions which greatly improved this manuscript. This research was partially funded by the Geological Society of London.

Appendix A. Supplementary data

The SA Calc software used to calculate structural anisotropy can be found online at https://github.com/beardyscientist/sa_calc.

Script and step-by-step guide can be found online at https://doi.org/10.1016/j.jsg.2019.103939.

References

Buchs, D.M., Baumgartner, P.O., Baumgartner-mora, C., Bandini, A.N., 2009. Late Cretaceous to Miocene seamount accretion and melange formation in the Osa and Burica Peninsulas (Southern Costa Rica): episodic growth of a convergent margin. Geol. Soc. Lond. Spec. Publ. 328, 411–456.

Buczek, M.B., Herakovich, C.T., 1985. A normal stress criterion for crack extension direction in orthotropic composite materials. J. Compos. Mater. 19, 544–553. https://doi.org/10.1177/002199838501900606.

Butler, R.W.H., Bond, C.E., Shipton, Z.K., Jones, R.R., Casey, M., 2008. Fabric anisotropy controls faulting in the continental crust. J. Geol. Soc. 165, 449–452. https://doi.org/10.1144/0016-76492007-129.

Button, E., Riedmüller, G., Schubert, W., Klima, K., Medley, E., 2004. Tunnelling in tectonic melanges?accommodating the impacts of geomechanical complexities and anisotropic rock mass fabrics. Bull. Eng. Geol. Environ. 63 https://doi.org/10.1007/s10064-003-0220-7.

Cladouhos, T.T., 1999. Shape preferred orientations of survivor grains in fault gouge. J. Struct. Geol. 21, 419–436. https://doi.org/10.1016/S0191-8141(98)00123-0.

Clarke, A.P., 2014. Discerning the Age of NW – SE Trending Mafic Dykes at Llanbadrig, N. Anglesey through Geochemical and Structural Analysis. Masters Thesis. University of Leicester.

Clarke, A.P., 2018. Heterogeneous Input in a Subduction System & its Effect on Plate Boundary Processes: Structural Analysis of the Osa Mélange, SW Costa Rica. Doctoral thesis. Royal Holloway, University of London.

Clarke, A.P., Vannucchi, P., Morgan, J., 2018. Seamount chain–subduction zone interactions: implications for accretionary and erosive subduction zone behavior. Geology 46, 367–370. https://doi.org/10.1130/G40063.1.

Coli, N., Berry, P., Boldini, D., Bruno, R., 2008. In Situ Large Size Non Conventional Shear Tests for the Mechanical Characterization of a Bimrock in the Santa Barbara Open Pit Mine (Italy).

Eden, C.P., Andrews, J.R., 1990. Middle to upper devonian melanges in SW Spain and their relationship to the meneage formation in south cornwall. In: *Proceedings of the Ussher Society* – Annual Conference of the Ussher Society, January 1990, pp. 217–222.

Forbes Inskip, N.D., Meredith, P.G., Chandler, M.R., Gudmundsson, A., 2018. Fracture properties of nash point shale as a function of orientation to bedding. J. Geophys. Res.: Solid Earth 123, 8428–8444. https://doi.org/10.1029/2018JB015943.

Fuentes, P., Díaz-Alvarado, J., Fernández, C., Díaz-Azpiroz, M., Rodríguez, N., 2016. Structural analysis and shape-preferred orientation determination of the mélange facies in the Chañaral mélange, Las Tórtolas Formation, Coastal Cordillera, northern Chile. J. South Am. Earth Sci. 67, 40–56. https://doi.org/10.1016/j.jsames.2016.02.001.

Gibbons, W., McCarroll, D., 1993. Geology of the Country Around Aberdaron, Including Bardsey Island. HMSO. British Geological Survey Memoirs Series.

Grigull, S., Krohe, A., Moos, C., Wassmann, S., Stöckhert, B., 2012. "Order from chaos": a field-based estimate on bulk rheology of tectonic mélanges formed in subduction zones. Tectonophysics 568–569, 86–101. https://doi.org/10.1016/j.tecto.2011.11.004.

Haneberg, W.C., 2004. Simulation of 3D Block Populations to Characterize Outcrop Sampling Bias in Bimrocks, vol. 8.

Herwegh, M., Handy, M.R., 1998. The origin of shape preferred orientations in mylonite: inferences from in-situ experiments on polycrystalline norcamphor. J. Struct. Geol. 20, 681–694. https://doi.org/10.1016/S0191-8141(98)00011-X.

Kano, K., Nakaji, M., Takeuchi, S., 1991. Asymmetrical melange fabrics as possible indicators of the convergent direction of plates: a case study from the Shimanto Belt of the Akaishi Mountains, central Japan. Tectonophysics 185, 375–388. https://doi.org/10.1016/0040-1951(91)90455-2.

Kawai, T., Windley, B.F., Terabayashi, M., Yamamoto, H., Isozaki, Y., Maruyama, S., 2008. Neoproterozoic glaciation in the mid-oceanic realm: an example from hemipelagic mudstones on Llanddwyn Island, Anglesey, UK. Gondwana Res. 14, 105–114. https://doi.org/10.1016/j.gr.2007.12.008.

Kim, C., Snell, C., Medley, E., 2004. Shear Strength of Franciscan Complex Melange as Calculated from Back-Analysis of a Landslide, vol. 8.

Launeau, P., Robin, P.-Y.F., 1996. Fabric analysis using the intercept method. Tectonophysics 267, 91–119. https://doi.org/10.1016/S0040-1951(96)00091-1.

Launeau, P., Robin, P.-Y.F., 2005. Determination of fabric and strain ellipsoids from measured sectional ellipses—implementation and applications. J. Struct. Geol. 27, 2223–2233. https://doi.org/10.1016/j.jsg.2005.08.003.

Lindquist, E.S., 1994. The Strength and Deformation Properties of Mélange. Ph.D. Thesis. Department of Civil Engineering, University of California, Berkeley.

Lindquist, E.S., Goodman, R.E., 1994. Strength and deformation properties of a physical model melange. In: ARMA-1994-0843 – 1st North American Rock Mechanics Symposium, vol. 8. ARMA, American Rock Mechanics Association.

Louis, L., David, C., Metz, V., Robion, P., Menéndez, B., Kissel, C., 2005. Microstructural control on the anisotropy of elastic and transport properties in undeformed sandstones. Int. J. Rock Mech. Min. Sci. 42, 911–923. https://doi.org/10.1016/j.ijrmms.2005.05.004.

Medley, E., 1994. The Engineering Characterization of Melanges and Similar Block-In-Matrix Rocks (Bimrocks). Doctoral thesis. University of California at Berkeley.

Medley, E.W., 1994. Using stereologic methods to estimate the block volumetric proportion in melanges and similar block-in-matrix rocks (bim- rocks). In: Proceedings of the Congress of the International Association of Engineering Geologists, 7th – 7th International IAEG Congress. A.A. Balkema, Lisbon, Portugal, Rotterdam, pp. 1031–1040.

Medley, E.W., 1997. Uncertainty in estimates of block volumetric proportions in melange bimrocks. In: Proceedings International Symposium on Engineering Geology and the Environment – Engineering Geology and the Environment.

Medley, E.W., 2002. Estimating Block Size Distributions of Melanges and Similar Block-In- Matrix Rocks (Bimrocks), vol. 8.

Medley, E.W., 2004. Observations on tortuous failure surfaces in bimrocks. Felsbau 22.

Medley, E.W., Lindquist, E.S., 1995. The engineering significance of the scale-independence of some franciscan melanges in California, USA. In: Rock Mechanics Proceedings of the 35th U.S. Symposium.

Medley, E.W., Zekkos, D., 2011. Geopractitioner approaches to working with antisocial mélanges. In: Geological Society of America Special Papers. Geological Society of America, pp. 261–277. https://doi.org/10.1130/2011.2480(13.

Raimbourg, H., Famin, V., Palazzin, G., Yamaguchi, A., Augier, R., 2017. Tertiary evolution of the Shimanto belt (Japan): a large-scale collision in early miocene: early miocene collision in Shimanto belt. Tectonics 36, 1317–1337. https://doi.org/10.1002/2017TC004529.

Raymond, L.A., 1984. Classification of melanges. In: Raymond, L.A. (Ed.), *Melanges: Their Nature, Origin, and Significance*. Geological Society of America.

Riedmüller, G., Brosch, F.J., Klima, K., Medley, E.W., 2001. Engineering geological characterization of brittle faults and classification of fault rocks. Felsbau 19, 8.

Roadifer, J.W., Forrest, M.P., Lindquist, E., 2009. Evaluation of shear strength of mélange foundation at calaveras dam. In: Proceedings of 29th US Society for Dams – Annual Meeting and Conference: "Managing Our Water Retention Systems", vol. 15. Nashville, Tennessee.

Robin, P.-Y.F., 2002. Determination of fabric and strain ellipsoids from measured sectional ellipses — theory. J. Struct. Geol. 24, 531–544. https://doi.org/10.1016/S0191-8141(01)00081-5.

Savage, M.K., 1999. Seismic anisotropy and mantle deformation: what have we learned from shear wave splitting? Rev. Geophys. 37, 65–106. https://doi.org/10.1029/98RG02075.

Shervais, J.W., Choi, S.H., Sharp, W.D., Ross, J., Zoglman-Schuman, M., Mukasa, S.B., 2011. Serpentinite matrix mélange: implications of mixed provenance for mélange formation. In: Geological Society of America Special Papers. Geological Society of America, pp. 1–30. https://doi.org/10.1130/2011.2480(01.

Silver, E.A., Beutner, E.C., 1980. Melanges. Geology 8, 32–34. https://doi.org/10.1130/0091-7613(1980)8<32:M>2.0.CO;2.

Singleton, J.S., Cloos, M., 2013. Kinematic analysis of mélange fabrics in the Franciscan Complex near San Simeon, California: evidence for sinistral slip on the Nacimiento fault zone? Lithosphere 5, 179–188. https://doi.org/10.1130/L259.1.

Sönmez, H., Gokceoglu, Candan, Tuncay, Ergün, Medley, Edmund W., Nefeslioglu, Hakan A., 2004. Relationships between volumetric block proportions and overall UCS of a volcanic bimrock. Felsbau 22, 27–34.

Suzuki, T., Hada, S., 1979. Cretaceous tectonic melange of the Shimanto belt in Shikoku, Japan. J. Geol. Soc. Jpn. 85, 467–479. https://doi.org/10.5575/geosoc.85.467.

Svitek, T., Vavryčuk, V., Lokajíček, T., Petružálek, M., 2014. Determination of elastic anisotropy of rocks from P- and S-wave velocities: numerical modelling and lab measurements. Geophys. J. Int. 199, 1682–1697. https://doi.org/10.1093/gji/ggu332.

Takesue, N., Suzuki, S., 2016. Prelithification Shear Structures of Mélange Unit in Shiofuki-Iwa Area, the Upper Cretaceous Shimanto Belt, vol. 23. Okayama University Earth Science Reports, Wakayama Prefecture, Japan, pp. 9–15.

Tepp, G., Gallacher, R., Accardo, N., Shillington, D.J., Gaherty, J., Keir, D., Nyblade, A. A., Mbogoni, G.J., Chindandali, P.R.N., Ferdinand-Wambura, R., Mulibo, G.D., Kamihanda, G., 2018. Seismic anisotropy of the upper mantle below the western rift, East Africa. J. Geophys. Res. Solid Earth 123 (7), 5644–5660. https://doi.org/10.1029/2017JB015409.

Vannucchi, P., Fisher, D.M., Bier, S., Gardner, T.W., 2006. From seamount accretion to tectonic erosion: formation of Osa Mélange and the effects of Cocos Ridge subduction in southern Costa Rica. Tectonics 25. https://doi.org/10.1029/2005TC001855 n/a-n/a.

Vannucchi, P., Morgan, J.P., Silver, E.A., Kluesner, J.W., 2016. Origin and Dynamics of Depositionary Subduction Margins, vol. 17. https://doi.org/10.1002/2016GC006259, 14217–14217.

Wakabayashi, J., 2008. Franciscan complex, California: problems in recognition of melanges, and the gap between research knowledge and professional practice. In: Proceedings, Conference of American Rock Mechanics Association. San Francisco, vol. 13.

Wood, M., 2012. The historical development of the term ‘mélange’ and its relevance to the precambrian geology of Anglesey and the Lleyn Peninsula in Wales, UK. J. Geogr. 121, 168–180. https://doi.org/10.5026/jgeography.121.168.